Atmospheric
Chemistry
and Physics
Discussions

Open Access

Sources, solubility, and acid processing of aerosol iron and phosphorous over the South China Sea: East Asian dust and pollution outflows vs. Southeast Asian biomass burning

S.-C. Hsu[1], G.-C. Gong[2], F.-K. Shiah[1,3], C.-C. Hung[4], S.-J. Kao[5], R. Zhang[6], W.-N. Chen[1], C.-C. Chen[7], C. C.-K. Chou[1], Y.-C. Lin[1], F.-J. Lin[3], and S.-H. Lin[1]

[1]Research Center for Environmental Changes (RCEC), Academia Sinica, Taipei, Taiwan, ROC
[2]Institute of Marine Environmental Chemistry and Ecology, National Taiwan Ocean University, Keelung, Taiwan
[3]Institute of Oceanography, National Taiwan University, Taipei, Taiwan, ROC
[4]Department of Oceanography, and Asia-Pacific Ocean Research Center, National Sun Yat-sen University, Kaohsiung, Taiwan
[5]State Key Laboratory of Marine Environmental Science, Xiamen University, Xiamen, China
[6]Key Laboratory of Regional Climate-Environment Research for Temperate East Asia, Institute of Atmospheric Physics, Chinese Academy of Sciences, Beijing, China

Title Page

Abstract	Introduction
Conclusions	References
Tables	Figures

|◄ | ►|
◄ | ►
Back | Close

Full Screen / Esc

Printer-friendly Version

Interactive Discussion

[7]Department of Life Science, National Taiwan Normal University, Taipei, Taiwan

Correspondence to: S.-C. Hsu (schsu815@rcec.sinica.edu.tw)

ACPD

14, 21433–21472, 2014

Sources, solubility, and acid processing of aerosol iron and phosphorous over the South China Sea

S.-C. Hsu et al.

Title Page

Abstract | Introduction

Conclusions | References

Tables | Figures

|◄ | ►|

◄ | ►

Back | Close

Full Screen / Esc

Printer-friendly Version

Interactive Discussion

S.-C. Hsu et al.

Abstract

Iron and phosphorous are essential to marine microorganisms in vast regions in oceans worldwide. Atmospheric inputs are important allochthonous sources of Fe and P. The variability in airborne Fe deposition is hypothesized to serve an important function in previous glacial–interglacial cycles, contributing to the variability in atmospheric CO_2 and ultimately the climate. Understanding the mechanisms underlying the mobilization of airborne Fe and P from insoluble to soluble forms is critical to evaluate the biogeochemical effects of these elements. In this study, we present a robust power-law correlation between fractional Fe solubility and non-sea-salt-sulfate/Total-Fe (nss-sulfate/Fe_T) molar ratio independent of distinct sources of airborne Fe of natural and/or anthropogenic origins over the South China Sea. This area receives Asian dust and pollution outflows and Southeast Asian biomass burning. This correlation is also valid for nitrate and total acids, demonstrating the significance of acid processing in enhancing Fe mobilization. Such correlations are also found for P, yet source dependent. These relationships serve as straightforward parameters that can be directly incorporated into available atmosphere–ocean coupling models that facilitate the assessment of Fe and P fertilization effects. Although biomass burning activity may supply Fe to the bioavailable Fe pool, pyrogenic soils are possibly the main contributors, not the burned plants. This finding warrants a multidisciplinary investigation that integrates atmospheric observations with the resulting biogeochemistry in the South China Sea, which is influenced by atmospheric forcings and nutrient dynamics with monsoons.

1 Introduction

Iron (Fe), a micronutrient to marine algae, is a limiting nutrient found in over one-third of oceans worldwide, particularly in high nitrate–low chlorophyll regions (Martin, 1990; Martin et al., 1994; Fung et al., 2000; Jickells et al., 2005). Fe, along with phospho-

Sources, solubility, and acid processing of aerosol iron and phosphorous over the South China Sea

S.-C. Hsu et al.

rus (P) and other potential trace elements, is also a (co)limiting nutrient of nitrogen (N) fixation in the oligotrophic areas of the ocean (Falkowski, 1997; Mills et al., 2004). The stimulation of these elements during phytoplankton growth and primary production is linked to carbon sequestration and, consequently, the changing climate through-
5 out the geologic time (Martin, 1990; Jickells et al., 2005). The open ocean is far from coasts with decreased influence by the riverine inputs. Hence, atmospheric supply is widespread and serves as a chief source of Fe and P in the vast oceanic regimes. However, only a portion of atmospheric particle-bound Fe and P dissolves upon deposition to the ocean surface, resulting in the bioavailability of these elements. The amounts
10 of Fe and P can be related to atmospheric, oceanic, and biological processes (Fung et al., 2000; Jickells et al., 2005; Mahowald et al., 2005; Baker and Croot, 2010; Rubin et al., 2011) as well as to the intrinsic properties and origins of the particles (Baker and Jickells, 2006; Sholkovitz et al., 2012; Shi et al., 2012). The following factors have been proposed to regulate the mobilization of Fe and P during atmospheric transport from
15 intrinsically insoluble to relatively soluble speciation: acid, cloud, and aging processes (the latter two processes are also involved with acid processing) (Zhuang et al., 1992; Meskhidze et al., 2003, 2005; Luo et al., 2005; Mackie et al., 2005; Solmon et al., 2009; Rubasinghege et al., 2010; Hsu et al., 2010a; Shi et al., 2011a, b; Ito and Xu, 2014); alkalinity neutralization (Ito and Feng, 2010); photochemistry (Zhu et al., 1997); and
20 organic complexation (Fu et al., 2010).

In addition to atmospheric processes, sources other than natural origins (mainly dust) also contribute to the abundance of atmospheric Fe and P in an industrial era. Globally, mineral dust contributes > 95 % (Luo et al., 2008) and 82 % (Mahowald et al., 2008) of Fe and P deposition, respectively. Nevertheless, anthropogenic sources, such
25 as fossil fuel combustion and biomass burning, may also exert to contributing more Fe and P in the present day regionally (Chuang et al., 2005; Guieu et al., 2005; Sholkovitz et al., 2009; Schroth et al., 2009). For example, Luo et al. (2008) suggested that combustion sources contribute approximately 30 % of the total Fe deposition in northwest Pacific close to the Asian continent. Previous studies have conducted single particle

analysis and observed a strong association between Fe-containing particles and anthropogenic species, such as sulfate, soot, black carbon, potassium (K), and anthropogenic metals, in the East Asian outflows, which suggests the dominance of coal combustion (Furutani et al., 2011; Moffet et al., 2012) and/or atmospheric processes (Sullivan et al., 2007). Phosphorus (and thus phosphate) from biomass burning and industrial sources through atmospheric deposition is an important source of new P in terrestrial and oceanic eco-environments, which can reach over 50 % in certain perturbed areas, impacting substantially biogeochemical cycling and in turn C stocks in ecosystems (Mahowald et al., 2005, 2008, 2009). Using three aerosol species, namely, aluminum (Al), black carbon (C), and K, as tracers for mineral dust, biomass burning, and primary biogenic particles, respectively, Mahowald et al. (2005) found that numerical models cannot very successfully simulate the relative contributions of these sources to the observed water-soluble P. This finding suggests that other factors, such as atmospheric processing, are also involved.

The contributions of natural dust vs. anthropogenic (including biomass burning) aerosols to soluble Fe and P, and the function of acid processing in modifying the two types of Fe/P-containing particles remain uncertain. Specifically, the water-soluble (assuming also bioavailable) Fe and P measured over remote oceans downwind the source regions of desert dust, anthropogenic pollutant, and biomass burning might be directly contributed by the intrinsically water-soluble speciation in particles (Chuang et al., 2005; Guieu et al., 2005; Sholkovitz et al., 2009; Schroth et al., 2009). Alternatively, they can be generated during the long-range transport by certain atmospheric processes, such as cloud, aging, and acid processing (Meskhidze et al., 2003, 2005; Luo et al., 2005; Mackie et al., 2005; Solmon et al., 2009; Hsu et al., 2010a, Shi et al., 2011a, b; Ito and Xu, 2014), which are associated with changes in size, mineralogy, and speciation (Baker and Jickells, 2006; Cwiertny et al., 2008; Journet et al., 2008; Shi et al., 2012). The South China Sea (SCS), the studied ocean, is the second largest marginal sea worldwide. Its subtropical northern part is influenced by the East Asian dust and pollution outflows (EADPOs) during the winter (northeasterly) monsoon (Hsu

et al., 2007, 2013a, 2014), and its tropical southern part is substantially affected by the Southeast Asian biomass burning (SEABB) during the summer monsoon (Lin et al., 2009). During the early 2013 (January and February), the majority of North China encompassing Beijing might have suffered from the historically most severe air pollution

⁵ with abnormally elevated PM$_{2.5}$ of over 600 µg m^{-3} (Quan et al., 2014). This severe air pollution elevated anthropogenic aerosol loadings within the marine boundary layer of the Chinese marginal seas, including the SCS, as revealed by a large satellite-retrieved fine aerosol optical depth of 0.3 to 0.5 (Fig. 1). Moderate-resolution imaging spectroradiometer (MODIS) images revealed that Indonesian biomass burning took place earlier

¹⁰ in June 2013 leading to the deterioration of air quality not only in Indonesia but also in Malaysia and Singapore (Betha et al., 2014) and over the surrounding SCS (Fig. 2). Marine aerosol samples were collected onboard over the SCS in early spring and June of 2013 (Fig. 3 and Table S1) when the atmosphere was influenced predominantly by EADPOs and SEABB, respectively. The water-soluble fractions and total fractions of

¹⁵ specific elements that can serve as micronutrients were measured. The present study covers a few challenging topics in terms of distinctive dissolution characteristics of airborne Fe and P associated with varying sources and their relative significance in supplying potentially bioavailable Fe and P to the SCS. To the best of our knowledge, this study is the first to analyze Fe and P solubility in the SCS and prove that acid

²⁰ processing enhances Fe and P dissolution regardless of their sources.

2   Materials and methods

Marine aerosol samples were collected on two cruises onboard the R/V *Oceanic Researcher V* (*OR5*) over the SCS. The first cruise was conducted over the northern SCS between 18 February and 8 March 2013 (Fig. 3a), and the second cruise was over the

²⁵ entire SCS between 17 and 30 June 2013 (Fig. 3b). The sampling oceanic region during the first cruise was influenced by EADPO (Figs. 1 and 4a), whereas that during the second cruise was influenced by SEABB (Figs. 2 and 4b). A total of 18 and 17

total suspended particulate (TSP) samples were collected on respective cruise. They were subject to analyses of total fraction of Al, Fe, and P (Al_T, Fe_T, and P_T) through microwave digestion pretreatment and water-soluble fraction of Al, Fe, and P (Al_S, Fe_S, and P_S) as well as major ions (SO_4^{2-}, NO_3^-, Cl^-, Na^+, Mg^{2+}, K^+, and Ca^{2+}) through Milli-Q water extraction. Detailed sampling and analytical procedures were adopted from previous studies (Hsu et al., 2010a, b, 2013a, 2014).

For the extraction, the derived fractional solubility of Fe using Milli-Q water may be relatively higher than that derived using seawater (Buck et al., 2006; Chen et al., 2006). However, Aguilar-Islas et al. (2010) obtained contrasting results. Based on the GEO-TRACES inter-laboratory comparison, Morton et al. (2013) recommended flow-through extraction as a standard protocol for determining water-soluble Fe and trace elements in aerosols. However, Hsu et al. (2013b) found that the resulting fractional solubility of refractory elements (Fe, Al, and Ti) obtained by the modified flow-through extraction is close to that acquired by common batch extraction. Accordingly, the present study adopted batch extraction to readily compare the present with previous results.

3   Results and discussion

3.1   Temporal and spatial distribution of Fe_T, Fe_S, P_T, and P_S over the SCS

Figure 5 depicts the time series of Fe_T, Fe_S, P_T, P_S, and other aerosol species (Al_T, non-sea-salt (nss)-SO_4^{2-}, nss-K^+, and NO_3^-) measured on the two ship cruises. Al_T, nss-SO_4^{2-}, and nss-K^+ are tracers of mineral dust, anthropogenic substance (particularly coal combustion), and biomass burning aerosol, respectively. A similar procedure was conducted by Mahowald et al. (2005). Overall, the concentrations of these species significantly varied during the two cruises, and the total fractions varied more remarkably than the water-soluble fractions (Table 1). In addition, the species mostly showed synchronous variations with few exceptional data, as supported by good correlations among all terrestrial species, except for sea spray species (Table 2). However, differ-

ent degrees of variability were observed in certain species. For instance, the increase in Fe_S and nss-SO_4^{2-} between 22 and 24 February was relatively dramatic compared with those in other species (Fig. 5a). On the February–March cruise, another peak occurred on 5 to 7 March when various species were raised. These two episodes were associated with EADPOs mainly from north and east China, driven by the prevailing northeastern winter monsoon, which can be demonstrated further by MODIS-retrieved aerosol optical depth distribution (Fig. 1) and trajectory analysis (Fig. 4).

On the June cruise, low concentrations for all selected species were observed on 17 to 19 June. When the sampling ship went into south of 16° N, the concentrations sharply increased and peaked on around 22 June (Fig. 5b). This pollution episode can be attributed to the extensive SEABB in Sumatra, Indonesia since mid-June, as demonstrated by the MODIS-retrieved fire spot distribution (Fig. 2). The resulting northward advection substantially deteriorated air quality over Malaysia and Singapore (Betha et al., 2014). During the first few days of this cruise, strong atmospheric disturbance prevailed over the northern SCS off western Philippine and subsequently formed a tropical depression on 20 June and then Typhoon Bebinca on 21 June. This typhoon further moved westward and made landfall over Hainan Island on 22 June (http://en.wikipedia.org/wiki/Timeline_of_the_2013_Pacific_typhoon_season). The disturbance might have disrupted the northward dispersion of biosmoke plume at that time, which led to low concentrations over the northern SCS on 17 June to 19. Therefore, the air masses collected during that period might represent the relatively clean background maritime airs in summer, distinct from those thereafter affected by Indonesian biosmoke, as illustrated by fire spot distribution retrieved by satellites and trajectory analysis (Figs. 2 and 4). This phenomenon gave rise to the elevation of aerosol species (Fig. 5b).

Table 1 statistically summarizes the data on the concentrations of selected species and solubility of Fe and P registered on the two cruises. The Fe_S concentrations (range: $11\,\mathrm{ng\,m^{-3}}$ to $56\,\mathrm{ng\,m^{-3}}$ and average: $23 \pm 17\,\mathrm{ng\,m^{-3}}$) over the northern SCS during the earlier springtime cruise were comparable with those (~ 5 to $\sim 90\,\mathrm{ng\,m^{-3}}$) observed

Sources, solubility, and acid processing of aerosol iron and phosphorous over the South China Sea

S.-C. Hsu et al.

Title Page

Abstract	Introduction
Conclusions	References
Tables	Figures

|◄ | ►|

◄ | ►

Back | Close

Full Screen / Esc

Printer-friendly Version

Interactive Discussion

in the northern East China Sea (ECS) (Chuang et al., 2005) and those (21 ± 22 and 31 ± 46 ng m^{-3} for the non-dusty and dusty northeastern monsoon, respectively) measured in spring over the ECS (Hsu et al., 2010a, b). Further comparison showed that the June samples also had Fe$_S$ concentrations nearly similar to those in the February–March samples. However, %Fe was significantly distinguishable, with considerably higher solubility in the February–March samples ($11\% \pm 5.3\%$) than in the June samples ($2.5\% \pm 1.5\%$, excluding the three background samples collected on the earlier days of the cruise) and even the ECS ($7.7\% \pm 4.5\%$). Similarly, the mean P$_S$ concentration (5.6 ± 4.7 ng m^{-3}) was close to that in the non-dusty spring (6.4 ± 6.1 ng m^{-3}) but lower than that in the dusty spring over the ECS (17 ng m^{-3}) (Hsu et al., 2010b). The June samples had virtually higher concentrations (16 ± 12 ng m^{-3}) than the February–March samples and were comparable with the samples measured over the dusty ECS. Meanwhile, %P was relatively constant in the February–March ($55\% \pm 14\%$) and June samples ($50\% \pm 14\%$). The %P in the former period in the SCS was close to that ($61\% \pm 22\%$) in the ECS (Hsu et al., 2010b). Such values are similar to the solubility ($\sim 50\%$) of P from anthropogenic sources (Mahowald et al., 2008).

Besides, it is noteworthy that Al$_T$, Fe$_T$, and P$_T$ concentrations were considerably higher in the June samples (1963 ± 914, 1212 ± 559, and 44 ± 19 ng m^{-3}, respectively) than in the February–March samples (212 ± 470, 205 ± 334, and 10 ± 11 ng m^{-3}, respectively), whereas nss-sulfate was higher in the February–March samples (6553 ± 3783 ng m^{-3}) than in the June samples (3681 ± 1570 ng m^{-3}). This finding indicates the distinct characteristics of air masses encountered. Unlike the former species, nitrate and nss-K$^+$ were comparable on the two cruises (3405 ± 2115 and 269 ± 118 ng m^{-3} for the February–March samples compared with 3351 ± 1039 and 262 ± 161 ng m^{-3} for the June samples). Compared with those acquired in the North Pacific (7.3 ± 4.3 and 2.5 ± 1.2 ng m^{-3} in the western and central North Pacific, respectively) (Furutani et al., 2010), the P$_T$ concentrations in the SCS were much higher, while it is noted that their cruises were conducted in summer. Further compared with those measured in the Sea

of Japan (average $23.7 \pm 24.4\,\mathrm{ng\,m^{-3}}$) (Kang et al., 2009), the summertime southern SCS was twice as much, but the late-wintertime northern SCS was 50 % lower.

3.2 Characteristic ratios of Fe and P against specific source tracers

In addition to several factors, such as particle size (surface area), minerals, and photo-
chemistry (Baker and Jickells, 2006; Baker and Croot, 2010; Shi et al., 2012), the main controlling factors of aerosol Fe and P dissolution include their intrinsic natures particularly in terms of sources/origins and speciation (Shi et al., 2011a; Guieu et al., 2005; Sedwick et al., 2007; Sholkovitz et al., 2009; Schroth et al., 2009; Trapp et al., 2010; Paris et al., 2013) and atmospheric processes that the Fe- and P-containing atmo-
spheric particles may experience during long-range transport (Meskhidze et al., 2003, 2005; Luo et al., 2005; Mackie et al., 2005; Fan et al., 2006; Solmon et al., 2009; Hsu et al., 2010a; Shi et al., 2011a, b; Takahashi et al., 2011; Ito and Xu, 2014). To explore the potential sources of Fe and P, Figs. 6 and 7 illustrate the correlations between Fe_T, Fe_S, P_T, and P_S against Al_T (or Al_S), nss-K^+, and nss-sulfate. The correlations of Fe_T
and P_T against Al_T were stronger than those of nss-K^+ and nss-sulfate against Fe_T and P_T (Fig. 6 and Table 2). The mean Fe_T/Al_T and P_T/Al_T mass ratios in marine aerosols for the February–March cruise (0.76 and 0.027) were slightly higher than those (0.62 and 0.022) for the June cruise. The Fe_T/Al_T ratio for the February–March cruise was consistent with those (0.45–0.82) extensively found in East Asian dust events (Arimoto
et al., 2006) but even slightly higher than that (~ 0.6) often found in springtime marine aerosols affected by East Asian dust plumes over the ECS and SCS (Hsu et al., 2010a, b, 2013). However, they are all comparable with those (0.68 and 0.013) in average crust composition (Taylor, 1964), suggesting the dominance of mineral dust for Fe_T and P_T. The observed Al_T maximum concentrations ($\sim 1200\,\mathrm{ng\,m^{-3}}$ to $1500\,\mathrm{ng\,m^{-3}}$)
were only half or less than those ($\sim 3000\,\mathrm{ng\,m^{-3}}$) typically found in spring (Hsu et al., 2008), and air pollution mainly arising from fossil fuel combustion usually reaches its maximum in winter in East and North China. Thus, this case might be a typical Asian

Title Page

Abstract | Introduction

Conclusions | References

Tables | Figures

|◄ | ►|

◄ | ►

Back | Close

Full Screen / Esc

Printer-friendly Version

Interactive Discussion

continental pollution outflow accompanied with weak dust. Aside from desert dust, the collected dust during the February–March cruise probably partially originated from anthropogenic sources rich in Fe, such as fly ash, industrial emissions, and urban fugitive dust (Zhang et al., 2013). Conversely, it is evident that extraordinary Al (and Fe) in June was relevant to Indonesian biomass burning, as found in other smoke plumes (Salam et al., 2003; Mkoma et al., 2009). However, Al mostly originated from resuspended pyrogenic soil dust rather than from burned plants because the latter alone cannot sustain such elevated Al (Gaudichet et al., 1995). Fe_T and P_T were dominated similarly by the resuspended soils based on their good correlations with Al_T and elemental ratios. The Fe_T concentrations were even higher than nss-K^+ (Fig. 6), leading to Fe_T/nss-K^+ ratios (2.9 ± 1.4) much higher than that (< 0.5) of biomass burning emission sources (Li et al., 2007; Schmidl et al., 2008). In the present study, the P_T/nss-K^+ ratio were 0.045 and 0.15 in the February–March and June samples, respectively. The latter observed in the Indonesian biomass burning plume is rather comparable with that (0.094, but for P_S/K^+) in Indonesian biomass burning aerosols (Engling et al., 2014). The total K in coarse aerosols was applied by Mahowald et al. (2005) as a tracer of primary biogenic particles, such as pollen, with a P/K ratio of 0.1375. According to the source profiles of $PM_{2.5}$ from coal combustion, P_T/K^+ ratios reached 0.6 to 5.2 (Watson et al., 2001), which is significantly larger than that (0.045) found in the EADPO plume. This finding probably implies the non-significant contribution of coal fly ash to P_T.

The mean Fe/Al ratios in soluble fraction (i.e., Fe_S/Al_S) increased to 1.63 in the February–March samples but slightly decreased to 0.43 in the June samples, with high correlation coefficients of > 0.95. This result might be attributed to the distinct aluminosilicate assemblages in EADPO and SEABB (Journet et al., 2008) and the differential dissolution capacities of Al and Fe (Buck et al., 2006). By contrast, the P/Al ratios in the two periods consistently sharply increased from ~ 0.025 in the total fraction (P_T/Al_T) to 0.40 and 0.32 in the soluble fraction (P_S/Al_S). This result obviously indicates that the solubility of P is considerably higher than that of Al. Both Fe_S and P_S correlated well with the three tracer species, implicating that mineral dust, fossil fuel combus-

Title Page

Abstract | Introduction

Conclusions | References

Tables | Figures

|◄ | ►|

◄ | ►

Back | Close

Full Screen / Esc

Printer-friendly Version

Interactive Discussion

tion, and biomass burning can be potential sources of Fe_S and P_S. Nevertheless, the Fe_S/nss-K^+, P_S/nss-K^+, Fe_S/nss-sulfate, and P_S/nss-sulfate ratios changed the order between datasets of the two cruises, with twice to seven times higher values for the June samples than the February–March samples. As an exception, the Fe_S/nss-K^+ ratios were mutually close (0.11 and 0.10). K was also enriched in biosmoke plumes from China dominated by coal combustion (Hsu et al., 2009), although it is often utilized as a biomass burning tracer. Neither the Fe_S and P_S concentrations nor these aforementioned inter-species ratios were higher in the February–March samples. Many studies have suggested that both Fe_S and P_S are dominated by biomass burning and/or fossil fuel combustion instead of mineral dust (Chuang et al., 2005; Guieu et al., 2005; Furutani et al., 2010, 2011), although desert dust can be globally dominant (Luo et al., 2008; Mahowald et al., 2008). Our results further revealed that the SEABB aerosols could contribute to Fe_S and P_S not less than the EADPO aerosols over the SCS. However, such an argument does not consider the potential function of atmospheric processes in modifying their dissolution properties (Luo et al., 2005; Nenes et al., 2011) and the likelihood that mineral dust might be their inherent primary sources of Fe_S and P_S. In summary, relying on good correlations among selected aerosol species alone cannot identify and discriminate their relative contributions.

Data on Fe_S measured in the SCS (the present study) and found in inland China (i.e., urban Nanjing and desert city, Dunhuang) (Wang et al., 2002; Duvall et al., 2008), Yellow Sea (Chuang et al., 2005), and the ECS (Hsu et al., 2010a, b) were compared. In spite of scarcity, results showed that Fe_S concentrations remained at a considerably constant level, with an approximate average of $\leq 20\,\mathrm{ng\,m^{-3}}$ to $25\,\mathrm{ng\,m^{-3}}$, across such wide extents. In addition, the %Fe data in ambient aerosols (though very limited) in inland China were only $\leq 1.7\,\%$ (Duvall et al., 2008). This area had abnormally high nss-sulfate and nitrate as well as dust concentrations but no elevated Fe_S. Pronounced pollution cannot significantly raise Fe_S concentrations, indicating that anthropogenic sources might not be a critical Fe_S source. Alternatively, although anthropogenic sources might contribute to Fe_T, they are still present in water-insoluble

forms/speciation. The latter suggestion agrees with the result that although coal fly ash prevalent in China is supposedly a vital source of anthropogenic Fe, its %Fe is only < 2 % even in diluted H_2SO_4 solution (pH ≤ 2) (Chen and Grassian, 2013). This value is not distinct from (and even lower than) those of aluminosilicate dust in acidic medium (Mackie et al., 2005; Cwiertny et al., 2008; Journet al., 2008). Moreover, the uniformity of Fe_S over the large extent in space could not be physically explained by the transport of dissolvable Fe alone, regardless of whether the dissolvable Fe was inherently of natural or anthropogenic origins, because dilution effects would contribute to its decline *en route*. Atmospheric processes, such as cloud, aging, and acid processing are vital mechanisms of enhancing the dissolution of aerosol Fe and P (Zhu et al., 1997; Meskhidze et al., 2003, 2005; Luo et al., 2005; Mackie et al., 2005; Fan et al., 2006; Solmon et al., 2009; Hsu et al., 2010a; Shi et al., 2011a, b; Takahashi et al., 2011; Ito and Xu, 2014). The former two processes are also involved in acidic processes. In the relevant studies on acid processing, they are mostly dependent on laboratory experiments and numerical simulations, in which acid/particle (or acid/dust) mixing ratio is often adopted as a central parameter (Meskhidze et al., 2003, 2005; Shi et al., 2011b; Hsu et al., 2013b).

3.3 Variability in fractional Fe solubility in relation to acidic processing

Acidic/aging process is often hypothesized as a mechanism in enhancing Fe and P mobilization. However, a corroboration of direct observational data on marine aerosol composition remains insufficient. In addition, the variable of SO_2/dust ratio has been used in numerical modeling as an alternative surrogate to explore Fe solubility (Meskhidze et al., 2003, 2005). In the present study, we found that the nss-sulfate/Fe_T and nss-sulfate/P_T molar ratios were well correlated with %Fe and %P, respectively, showing positive power-law relationships, with higher R2 for Fe (0.93 and 0.84) than for P (0.61 and 0.45) (Fig. 8). Such correlation is also valid for nitrate (i.e., nitrate/Fe_T molar ratio vs. %Fe and nitrate/P_T molar ratio vs. %P; Fig. 9). Thus, the combination of nss-sulfate and nitrate that usually are the two main acidic (anionic) constituents of

atmospheric aerosols were further examined. Close correlations were again detected (i.e., Σ(nss-sulfate + nitrate)/Fe_T molar ratio vs. %Fe and Σ(nss-sulfate + nitrate)/P_T molar ratio vs. %P; Fig. 10). It is noteworthy that Fe and P behaved in distinct manners. Fe, even dominated likely by distinct sources in the two regions/seasons, followed

5   a similar tendency. Thus, the two regression curves could be merged as a whole, with a better R2 of 0.92. By contrast, the P in the two seasons/areas followed two regression curves. The underlying reasons for the observed discrepancy could be ascribed to the discernible dominance of their respective various sources vs. their susceptibility to acidic processes. For instance, the collected Fe and P originated from either more

10 aged East Asian dust plus anthropogenic aerosols in the late winter–early spring or relatively fresh biomass burning (mostly pyrogenic soils and partly burned plant) particles in June. Most Fe-bearing particles can be found in refractory (crystalline) minerals, such as goethite, hematite, and clay (Journet et al., 2008). Compared with Fe, P is originally associated within relatively poorly crystalline (or labile) minerals, such as apatite

15 [$Ca_3 (PO_4)_2$] in dust and organic matter in biomass burning, of which the latter has intrinsically higher solubility than the former (Paytan and McLaughlin, 2007). Fe- and P-containing particles from North China have traversed a few days (5 d to 7 d) to the SCS (Hsu et al., 2013a) so that they have sufficient time to react with acid substances in anthropogenic plumes *en route* (Zhang and Iwasak, 1999; Meskhidze et al., 2005;

20 Luo et al., 2005; Sullivan et al., 2007; Hsu et al., 2014; Ito et al., 2014). This phenomenon increased the nss-sulfate/Fe_T and nss-sulfate/P_T ratios in the springtime samples partly because of the formation of iron sulfate (Oakes et al., 2012). The collected Indonesian biomass burning aerosols containing Fe and P are relatively fresh, without sufficient time to react with reactive gases (e.g., SO_2 and HNO_3) in advecting

25 smoke (Baker et al., 2006; Srinivas and Sarin, 2012), leading to lower nss-sulfate/Fe_T and nss-sulfate/P_T ratios (and in turn %Fe and %P) in the June samples. Various sources might govern the initial solubilities of P and Fe, which is more critical for P than for Fe. Acid/aging process renders profound effects on the strengthened weathering of intrinsically refractory minerals, which is more helpful for Fe than for P.

Title Page

Abstract   Introduction

Conclusions   References

Tables   Figures

|◄   ►|

◄   ►

Back   Close

Full Screen / Esc

Printer-friendly Version

Interactive Discussion

In addition, HCl might also be important in the acidification of Fe-containing dust (Zhang et al., 2001); particularly, it is often elevated in smoke plumes. This effect cannot be readily evaluated because the Cl^- of sea salt-dominated aerosols in the marine boundary layer often suffers from profound Cl^- deficiency resulting from the heterogeneous reaction between sea salt particle and gaseous HNO_3 (Finlayson-Pitts and Hemminger, 2000; Hsu et al., 2007). The February–March samples had Cl^-/Na^+ mass ratios of ~ 1.45, which was lower than the characteristic ratio (1.80) of seawater. By contrast, excessive Cl^- (Ex-Cl^-) was observed in the June samples (bar charts in Fig. 5b). That is, these samples contained an excessive amount of Cl^- relative to the amount that the sea salt particles can sustain. This finding reveals the presence of biomass burning substances, which might be KCl or product of reaction between HCl released by biomass burning with alkaline/basic particles/chemicals, such as carbonate and (hydro)oxide minerals (Li et al., 2003). Moreover, we identified a diurnal trend from our limited diel samples (four days) in the last 3 d with higher Cl^- in daytime. This finding can be related to photochemistry. Nevertheless, no significant correlation existed between Ex-Cl^-/Fe_T and %Fe or between Ex-Cl^-/P_T and %P (not shown). The function of Cl^- (and/or HCl) in aerosol Fe and P acidification warrants further investigations.

Nss-sulfate and nitrate are secondary constituents through the gas-to-particle process. Good correlations between the secondary and primary species (dust, anthropogenic, and BB particles) indicate that their acidic precursor gases (SO_2 and NO_x) must have undergone a certain chemical process (i.e., heterogeneous reaction) to associate intimately with the primary particles *en route* (Seinfeld et al., 2004; Toboa et al., 2010; Hsu et al., 2014)., which has been demonstrated in dust and biomass burning plumes (Galy-Lacaux et al., 2001; Sullivan et al., 2007). The Acids/Fe_T ratio preferentially increased with time (or transported away from the source region). This finding might also be valid to some extent for Acids/P_T ratio. Therefore, the horizontal axis (Acids/Fe_T ratio) on Figs. 8 to 10 might represent the transporting distance (traveling time) and, consequently, aging degree. Several studies have employed the sum of nss-

sulfate and nitrate molar concentrations to define aerosol acidity (Buck et al., 2006). Fe content is usually close to that of Ca in mineral dust, which serves as a main neutralizer of dust aerosol acidity. Accordingly, the index Acids/Fe_T ratio approximates the acid/basic ratio, which represents the acidification degree of aerosols.

4   Implications and concluding remarks

In this study, we investigated the enhancing effect of acidification on aerosol Fe and P dissolution during atmospheric long-range transport. The %Fe (%P) had a robust (modest) power-law relationship with the nss-SO_4^{2-}/Fe_T (nss-SO_4^{2-}/P_T) molar ratio, which could thus be readily parameterized in atmosphere–ocean coupled models. Nevertheless, field and laboratory experiments have shown that organic acids might also promote the acid mobilization of dust Fe and P (Okada et al., 2006; Luo and Gao, 2010). For example, the presence of organic ligands, such as oxalate, can enhance the mobilization of Fe via complexion (Chen and Grassian, 2013). However, this result warrants further investigations. Moreover, our study considered other novel findings that might have been overlooked. First, the increased Fe_S observed in the biomass burning plumes were originated primarily from burned soils uplifted out of firing areas, called as pyrogenic soils, and likely not much from burned plants themselves. This condition might also be true for other oceans at times. Second, considering that biomass burning activities are highly prominent throughout the year in Southeast Asia surrounding the southern SCS, the results imply that the southern SCS might unexpectedly receive certain amounts of bioavailable Fe, presumably at least comparable to (or more than) the northern SCS. Moreover, available atmospheric numerical models may have largely underestimated eolian deposition of bioavailable Fe and P to the southern SCS, which is overwhelmed by biomass burning (i.e., biomass burning aerosols and pyrogenic soils). Aside from supplying macronutrients to the ecosystem, pyrogenic soils might also serve significant functions in the climate locally and regionally. Our results implicate anthropogenic activities in terms of acid pollutant emissions, and their future

mitigation would in turn change the supply of eolian water-soluble Fe and P. Another implication is that biogenic DMS emission and volcanic SO_2 explosion would play a role in dust Fe mobilization more crucial in the past than in the present. This study underscores the need for long-term measurements not only on the physicochemical and
5 optical properties of marine aerosols but also on atmospheric deposition.

In view of ocean biogeochemistry, the majority of the semi-closed SCS is nearly oligotrophic, and nitrogen fixation might account for a significant fraction of allochthonous nitrogen sources and new production in the SCS (Chou et al., 2006; Gaye et al., 2009; Kao et al., 2012). Fe and P are co-limiting nutrients of nitrogen fixation in the olig-
10 otrophic North Atlantic Ocean (Mills et al., 2004) and are also potentially critical for nitrogen fixation in the SCS (Wong et al., 2002; Wu et al., 2003; Gaye et al., 2009), while lacking a quantitative evaluation of these elements. Through remote sensing, Lin et al. (2009) found good correlations between satellite-retrieved aerosol optical depth and chlorophyll a in the central SCS. They attributed this finding to atmospheric depo-
15 sition. A significant difference in Fe_S/P_S molar ratio was detected between the EADPO (i.e., 2.3 ± 0.7) and the SEABB (i.e., 0.8 ± 0.2) plumes. Moreover, the $N_{Nitrate}:P$ ratios were significantly higher in the EADPO samples (i.e., ~ 300) than in the SEABB samples (i.e., ~ 75). The $N:P$ ratios were doubled after further considering the contributions of ammonium. Prolonged interaction of deposited aerosols in surface seawater
20 might amplify the P dissolution (Mackey et al., 2012), which could compensate the effect because of the addition of ammonium, thereby allowing the $N:P$ ratio to remain relatively stable. Together, the resulting biogeochemical effects in the SCS warrant further investigations. In addition to the SCS, the Indonesian biomass burning plumes would also extend toward the tropical/subtropical Indian and Pacific Oceans (Ott et al.,
25 2010). Therefore, the resulting oceanic impacts also need more attention (Krishnamurthy et al., 2009). In summary, our studies discussed a wide range of critical implications with respect to atmospheric chemistry and ocean biogeochemistry, which are worthy of further multidisciplinary investigations.

The Supplement related to this article is available online at doi:10.5194/acpd-14-21433-2014-supplement.

References

Aguilar-Islas, A. M., Wu, J., Rember, R., Johansen, A. M., and Shank, L. M.: Dissolution of aerosol-derived iron in seawater: leach solution chemistry, aerosol type, and colloidal iron fraction, Mar. Chem., 120, 25–33, 2010.

Arimoto, R., Kim, Y. J., Kim, Y. P., Quinn, P. K., Bates, T. S., Anderson, T. L., Gong, S., Uno, I., Chin, M., Huebert, B. J., Clarke, A. D., Shinozuka, Y., Weber, R. J., Anderson, J. R., Guazzotti, S. A., Sullivan, R. C., Sodeman, D. A., Prather, K. A., and Sokolik, I. N.: Characterization of Asian dust during ACE-Asia, Global Planet. Change, 52, 23–56, 2006.

Baker, A. R. and Croot, P. L.: Atmospheric and marine controls on aerosol iron solubility in seawater, Mar. Chem., 120, 4–13, 2010.

Baker, A. R. and Jickells, T. D.: Mineral particle size as a control on aerosol iron solubility, Geophys. Res. Lett., 33, L17608, doi:10.1029/2006GL026557, 2006.

Baker, A. R., French, M., and Linge, K. L.: Trends in aerosol nutrient solubility along a west–east transect of the Saharan dust plume, Geophys. Res. Lett., 33, L07805, doi:10.1029/2005GL024764, 2006.

Betha, R., Behera, S. N., and Balasubramanian, R.: Southeast Asian smoke haze: fractionation of particulate-bound elements and associated health risk, Environ. Sci. Technol., 48, 4327–4335, doi:10.1021/es405533d, 2014.

Buck, C. S., Landing, W. M., Resing, J. A., and Lebon, G. T.: Aerosol iron and aluminum solubility in the northwest Pacific Ocean: results from the 2002 IOC cruise, Geochem. Geophy. Geosy., 7, Q04M07, doi:10.1029/2005GC000977, 2006.

Chen, H. and Grassian, V. H.: Iron dissolution of dust source materials during simulated acidic processing: the effect of sulfuric, acetic, and oxalic acids, Environ. Sci. Technol., 47, 10312–10321, 2013.

Chen, Y., Street, J., and Paytan, A.: Comparison between pure-water-and seawater-soluble nutrient concentrations of aerosols from the Gulf of Aqaba, Mar. Chem., 101, 141–152, 2006.

Chou, W. C., Chen, Y.-L. L., Sheu, D. D., Shih, Y. Y., Han, C. A., Cho, C. L., Tseng, C. M., and Yang, Y. J.: Estimated net community production during the summertime at the SEATS time-series study site, northern South China Sea: implications for nitrogen fixation, Geophys. Res. Lett., 33, L22610, doi:10.1029/2005GL025365, 2006.

Chuang, P. Y., Duvall, R. M., Shafer, M. M., and Schauer, J. J.: The origin of water soluble particulate iron in the Asian atmospheric outflow, Geophys. Res. Lett., 32, L07813, doi:10.1029/2004GL021946, 2005.

Cwiertny, D. M., Baltrusaitis, J., Hunter, G. J., Laskin,A., Scherer, M. M., and Grassian, V. H.: Characterization and acid-mobilization study of iron-containing mineral dust source materials, J. Geophys. Res., 113, D05202, doi:10.1029/2007JD009332, 2008.

Duvall, R. M., Majestic, B. J., Shafer, M. M., Chuang, P. Y., Simoneit, B. R. T., and Schauer, J. J.: The water-soluble fraction of carbon, sulfur, and crustal elements in Asian aerosols and Asian soils, Atmos. Environ., 42, 5872–5884, 2008.

Engling, G., He, J., Betha, R., and Balasubramanian, R.: Assessing the regional impact of indonesian biomass burning emissions based on organic molecular tracers and chemical mass balance modeling, Atmos. Chem. Phys., 14, 8043–8054, doi:10.5194/acp-14-8043-2014, 2014.

Falkowski, P. G.: Evolution of the nitrogen cycle and its influence on the biological sequestration of CO_2 in the ocean, Nature, 387, 272–275, 1997.

Fan, S. M., Moxim, W. J., and Levy II, H.: Aeolian input of bioavailable iron to the ocean, Geophys. Res. Lett., 33, L07602, doi:10.1029/2005GL024852, 2006.

Finlayson-Pitts, B. J. and Hemminger, J. C.: Physical chemistry of airborne sea-salt particles and their components, J. Phys. Chem. A, 104, 11463–11477, 2000.

Fu, H., Cwiertny, D. M., Carmichael, G. R., Scherer, M. M., and Grassian, V. H.: Photoreductive dissolution of Fe–containing mineral dust particles in acidic media, J. Geophys. Res., 115, D11304, doi:10.1029/2009JD012702, 2010.

Fung, I. Y., Meyn, S. K., Tegen, I., Doney, S. C., John, J. G., and Bishop, J. K. B.: Iron supply and demand in the upper ocean, Global Biogeochem. Cy., 14, 281–295, 2000.

Furutani, H., Meguro, A., Iguchi, H., and Uematsu, M.: Geographical distribution and sources of phosphorus in atmospheric aerosol over the North Pacific Ocean, Geophys. Res. Lett., 37, L03805, doi:10.1029/2009GL041367, 2010.

Furutani, H., Jung, J., Miura, K., Takami, A., Kato, S., Kajii, Y., and Uematsu, M.: Single-particle chemical characterization and source apportionment of iron-containing atmospheric aerosols in Asian outflow, J. Geophys. Res., 116, D18204, doi:10.1029/2011JD015867, 2011.

Galy-Lacaux, C., Carmichael, G. R., Song, C. H., Lacaux, J. P., Al Ourabi, H., and Modi, A. I.: Heterogeneous processes involving nitrogenous compounds and Saharan dust inferred from measurements and model calculations, J. Geophys. Res., 106, 12559–12578, 2001.

Gaudichet, A., Echalar, F., Chatenet, B., Quisefit, J. P., Malingre, G., Cachier, H., Buat-Menard, P., Artaxo, P., and Maenhaut, W.: Trace elements in tropical African savanna biomass burning aerosols, J. Atmos. Chem., 22, 19–39, 1995.

Gaye, B., Wiesner, M. G., and Lahajnar, N.: Nitrogen sources in the South China Sea, as discerned from stable nitrogen isotopic ratios in rivers, sinking particles, and sediments, Mar. Chem., 114, 72–85, 2009.

Guieu, C., Bonnet, S., Wagener, T., and Loÿe-Pilot, M.-D.: Biomass burning as a source of dissolved iron to the open ocean?, Geophys. Res. Lett., 32, L19608, doi:10.1029/2005GL022962, 2005.

Hsu, S. C., Liu, S. C., Kao, S. J., Jeng, W. L., Huang, Y. T., Tseng, C. M., Tsai, F., Tu, J. Y., and Yang, Y.: Water-soluble species in the marine aerosol from the northern South China Sea: high chloride depletion related to air pollution, J. Geophys. Res., 112, D19304, doi:10.1029/2007JD008844, 2007.

Hsu, S. C., Liu, S. C., Huang, Y. T., Lung, C. S. C., Kao, S. J., Tsai F., and Tu, J. Y.: A criterion for identifying Asian dust events based on Al concentration data collected from northern Taiwan between 2002 and early 2007, J. Geophys. Res., 113, D18306, doi:10.1029/2007JD009574, 2008.

Hsu, S. C., Liu, S. C., Huang, Y. T., Chou, C. C. K., Lung, S. C. C., Liu, T. H., Tu, J. Y., and Tsai, F.: Long-range southeastward transport of Asian biosmoke pollution: signa-

Title Page

Abstract | Introduction

Conclusions | References

Tables | Figures

|◄ | ►|

◄ | ►

Back | Close

Full Screen / Esc

Printer-friendly Version

Interactive Discussion

ture detected by aerosol potassium in Northern Taiwan, J. Geophys. Res., 114, D14301, doi:10.1029/2009JD011725, 2009.

Hsu, S. C., Liu, S. C., Arimoto, R., Shiah, F. K., Gong, G. C., Huang, Y. T., Kao, S. J., Chen, J. P. Lin, F. J., Lin, C. Y., Huang, J. C., Tsai, F., and Lung, S. C. C.: Effects of acidic processing, transport history, and dust and sea salt loadings on the dissolution of iron from Asian dust, J. Geophys. Res., 115, D19313, doi:10.1029/2009JD013442, 2010a.

Hsu, S. C., Wong, T. F. G., Gong, G. C., Shiah, F. K., Huang, Y. T., Kao, S. J., Tsai, F., Lung, C. S. C., Lin, F. J., Lin, I. I., Hung, C. C., and Tseng, C. M.: Sources, solubility, and dry deposition of aerosol trace elements over the East China Sea, Mar. Chem., 120, 116–127, 2010b.

Hsu, S. C., Tsai, F., Lin, F. J., Chen, W. N., Shiah, F. K., Huang, J. C., Chan, C. Y., Chen, C. C., Liu, T. H., Chen, H. Y., Tseng, C. M., Huang, G. W., Huang, C. H., Lin, S. H., and Huang, Y. T.: A super Asian dust storm over the East and South China Seas: disproportionate dust deposition, J. Geophys. Res., 118, 7169–7181, doi:10.1002/jgrd.50405, 2013a.

Hsu, S. C., Lin, F. J., Liu, T. H., Lin, S. H., Kao, S. J. Tseng, C. M., and Huang, C. H.: Short time dissolution kinetics of refractory elements Fe, Al, and Ti in Asian outflow-impacted marine aerosols and implications, Atmos. Environ., 79, 93–100, 2013b.

Hsu, S. C., Lee, C. S. L., Huh, C. A., Shaheen, R., Lin, F. J., Liu, S. C., Liang, M. C., and Tao, J.: Ammonium deficiency caused by heterogeneous reactions during a super Asian dust episode, J. Geophys. Res., 119, 6803–6817, doi:10.1002/2013JD021096, 2014.

Ito, A. and Feng, Y.: Role of dust alkalinity in acid mobilization of iron, Atmos. Chem. Phys., 10, 9237–9250, doi:10.5194/acp-10-9237-2010, 2010.

Ito, A. and Xu, L.: Response of acid mobilization of iron-containing mineral dust to improvement of air quality projected in the future, Atmos. Chem. Phys., 14, 3441–3459, doi:10.5194/acp-14-3441-2014, 2014.

Jickells, T. D., An, Z. S., Andersen, K. K., Baker, A. R., Bergametti, G., Brooks, N., Cao, J. J., Boyd, P. W., Duce, R. A., Hunter, K. A., Kawahata, H., Kubilay, N., laRoche, J., Liss, P. S., Mahowald, N., Prospero, J. M., Ridgwell, A. J., Tegen, I., and Torres, R.: Global iron connections between desert dust, ocean biogeochemistry, and climate, Science, 308, 67–71, 2005.

Journet, E., Desboeufs, K. V., Caquineau, S., and Colin, J.-L.: Mineralogy as a critical factor of dust iron solubility, Geophys. Res. Lett., 35, L07805, doi:10.1029/2007GL031589, 2008.

Sources, solubility, and acid processing of aerosol iron and phosphorous over the South China Sea

S.-C. Hsu et al.

Title Page

Abstract	Introduction
Conclusions	References
Tables	Figures

|◄ | ►|

| ◄ | ► |

| Back | Close |

Full Screen / Esc

Printer-friendly Version

Interactive Discussion

Kang, J., Choi, M. S., and Lee, C. B.: Atmospheric metal and phosphorus concentrations, inputs, and their biogeochemical significances in the Japan/East Sea, Sci. Total Environ., 407, 2270–2284, 2009.

Kao, S. J., Yang, J.-Y. T., Liu, K. K., Dai, M., Chou, W.-C., Lin, H.-L., and Ren, H.: Isotope constraints on particulate nitrogen source and dynamics in the upper water column of the oligotrophic South China Sea, Global Biogeochem. Cy., 26, GB2033, doi:10.1029/2011GB004091, 2012.

Krishnamurthy, A., Moore, J. K., Mahowald, N., Luo, C., Doney, S. C., Lindsay, K., and Zender, C. S.: Impacts of increasing anthropogenic soluble iron and nitrogen deposition on ocean biogeochemistry, Global Biogeochem. Cy., 23, GB3016, doi:10.1029/2008GB003440, 2009.

Li, J., Pósfai, M., Hobbs, P. V., and Buseck, P. R.: Individual aerosol particles from biomass burning in southern Africa: 2. Compositions and aging of inorganic particles, J. Geophys. Res., 108, 8484, doi:10.1029/2002JD002310, 2003.

Li, X., Wang, S., Duan, L., Hao, J., Chao, L., Chen, Y., and Yang, L.: Particulate and trace gas emissions from open burning of wheat straw and corn stover in China, Environ. Sci. Technol., 41, 6052–6058, 2007.

Lin, I.-I., Wong, G. T. F., Lien, C.-C., Chien, C.-Y., Huang, C.-W., and Chen, J.-P.: Aerosol impact on the South China Sea biogeochemistry: an early assessment from remote sensing, Geophys. Res. Lett., 36, L17605, doi:10.1029/2009GL037484, 2009.

Luo, C. and Gao, Y.: Aeolian iron mobilisation by dust-acid interactions and their implications for soluble iron deposition to the ocean: a test involving potential anthropogenic organic acidic species, Environ. Chem., 7, 153–161, 2010.

Luo, C., Mahowald, N. M., Meskhidze, N., Chen, Y., Siefert, R. L., Baker, A. R., and Johansen, A. M.: Estimation of iron solubility from observations and a global aerosol model, J. Geophys. Res., 110, D23307, doi:10.1029/2005JD006059, 2005.

Luo, C., Mahowald, N., Bond, T., Chuang, P. Y., Artaxo, P., Siefert, R., Chen, Y., and Schauer, J.: Combustion iron distribution and deposition, Global Biogeochem. Cy., 22, GB1012, doi:10.1029/2007GB002964, 2008.

Mackey, K. R. M., Roberts, K., Lomas, M. W., Saito, M. A., Post, A. F., and Paytan, A.: Enhanced solubility and ecological impact of atmospheric phosphorus deposition upon extended seawater exposure, Environ. Sci. Technol., 46, 10438–10446, 2012.

Mackie, D. S., Boyd, P. W., Hunter, K. A., and McTainsh, G. H.: Simulating the cloud processing of iron in Australian dust: pH and dust concentration, Geophys. Res. Lett., 32, L06809, doi:10.1029/2004GL022122, 2005.

Mahowald, N. M., Artaxo, P., Baker, A. R., Jickells, T. D., Okin, G. S., Randerson, J. T., and Townsend, A. R.: Impacts of biomass burning emissions and land use change on Amazonian atmospheric phosphorus cycling and deposition, Global Biogeochem. Cy., 19, GB4030, doi:10.1029/2005GB002541, 2005.

Mahowald, N., Jickells, T. D., Baker, A. R., Artaxo, P., Benitez-Nelson, C. R., Bergametti, G., Bond, T. C., Chen, Y., Cohen, D. D., Herut, B., Kubilay, N., Losno, R., Luo, C., Maenhaut, W., McGee, K. A., Okin, G. S., Siefert, R. L., and Tsukuda, S.: Global distribution of atmospheric phosphorus sources, concentrations and deposition rates, and anthropogenic impacts, Global Biogeochem. Cy., 22, GB4026, doi:10.1029/2008GB003240, 2008.

Mahowald, N. M., Engelstaedter, S., Luo, C., Sealy, A., Artaxo, P., Benitez-Nelson, C., Bonnet, S., Chen, Y., Chuang, P. Y., Cohen, D. D., Dulac, F., Herut, B., Johansen, A. M., Kubilay, N., Losno, R., Maenhaut, W., Paytan, A., Prospero, J. A., Shank, L. M., and Siefert, R. L.: Atmospheric iron deposition: global distribution, variability, and human perturbations, Annu. Rev. Marine Sci., 1, 245–278, 2009.

Martin, J. H.: Glacial–interglacial CO_2 change: the iron hypothesis, Paleoceanography, 5, 1 –13, 1990.

Martin, J. H., Coale, K. H., Johnson, K. S., Fitzwater, S. E., Gordon, R. M., Tanner, S. J., Hunter, C. N., Elrod, V. A., Nowicki, J. L., Coley, T. L., Barber, R. T., Lindley, S., Watson, A. J., Scoy, K. V., Law, C. S., Liddicoat, M. I., Ling, R., Stanton, T., Stockel, J., Collins, C., Anderson, A., Bidigare, R., Ondrusek, M., Latasa, M., Millero, F. J., Lee, K., Yao, W., Zhang, J. Y., Friederich, G., Sakamoto, C., Chavez, F., Buck, K., Kolber, Z., Greene, R., Falkowski, P., Chisholm, S. W., Hoge, F., Swift, R., Yungel, J., Turner, S., Nightingale, P., Hatton, A., Liss, P., and Tindale, N. W.: Testing the iron hypothesis in ecosystems of the equatorial Pacific Ocean, Nature, 371, 123–129, 1994.

Meskhidze, N., Chameides, W. L., Nenes, A., and Chen, G.: Iron mobilization in mineral dust: can anthropogenic SO_2 emissions affect ocean productivity? Geophys. Res. Lett., 30, 2085, doi:10.1029/2003GL018035, 2003.

Meskhidze, N., Chameides, W. L., and Nenes, A.: Dust and pollution: a recipe for enhanced ocean fertilization?, J. Geophys. Res., 110, D03301, doi:10.1029/2004JD005082, 2005.

Sources, solubility, and acid processing of aerosol iron and phosphorous over the South China Sea

S.-C. Hsu et al.

Title Page

Abstract	Introduction
Conclusions	References
Tables	Figures

|◄ | ►|

◄ | ►

Back | Close

Full Screen / Esc

Printer-friendly Version

Interactive Discussion

Mills, M. M., Ridame, C., Davey, M., La Roche, J., and Geider, R. J.: Iron and phosphorus co-limit nitrogen fixation in the eastern tropical North Atlantic, Nature, 429, 292–232, 2004.

Mkoma, S. L., Maenhaut, W., Chi, X., Wang, W., and Raes, N.: Characterisation of PM_{10} atmospheric aerosols for the wet season 2005 at two sites in East Africa, Atmos. Environ., 43, 631–639, 2009.

Moffet, R. C., Furutani, H., Rödel, T. C., Henn, T. R., Sprau, P. O., Laskin, A., Uematsu, M., and Gilles, M. K.: Iron speciation and mixing in single aerosol particles from the Asian continental outflow, J. Geophys. Res., 117, D07204, doi:10.1029/2011JD016746, 2012.

Morton, P. L., Landing, W. M., Hsu, S. C., Milne, A., Aguilar-Islas, A. M., Baker, A. R., Buck, C. S., Gichuki, S., Hasings, M., Hatta, M., Johansen, A. M., Losno, R., Mead, C., Patey, M., Swarr, G., Van Der Merwe, P., Vandermark, A., and Zamora, L. M.: Results from the 2008 GEOTRACES aerosol intercalibration study, Limnol. Oceanogr. Meth., 11, 62–78, 2013.

Nenes, A., Krom, M. D., Mihalopoulos, N., Van Cappellen, P., Shi, Z., Bougiatioti, A., Zarmpas, P., and Herut, B.: Atmospheric acidification of mineral aerosols: a source of bioavailable phosphorus for the oceans, Atmos. Chem. Phys., 11, 6265–6272, doi:10.5194/acp-11-6265-2011, 2011.

Oakes, M., Ingall, E. D., Lai, B., Shafer, M. M., Hays, M. D., Liu, Z. G., Russell, A. G., and Weber, R. J.: Iron solubility related to particle sulfur content in source emission and ambient fine particles, Environ. Sci. Technol., 46, 6637–6644, 2012.

Okada, K., Kuroki, Y., Makama, Y., Arakaki, T., and Tanahara, A.: Wavelength dependence of Fe(II) photoformation in the water-soluble fraction of aerosols collected in Okinawa, Japan, Environ. Sci. Technol., 40, 7790–7795, 2006.

Ott, L., Duncan, B., Pawson, S., Colarco, P., Chin, M., Randles, C., Diehl, T., and Nielsen, E.: Influence of the 2006 Indonesian biomass burning aerosols on tropical dynamics studied with the GEOS-5 AGCM, J. Geophys. Res., 115, D14121, doi:10.1029/2009JD013181, 2010.

Paris, R., Desboeufs, K. V., Formenti, P., Nava, S., and Chou, C.: Chemical characterisation of iron in dust and biomass burning aerosols during AMMA-SOP0/DABEX: implication for iron solubility, Atmos. Chem. Phys., 10, 4273–4282, doi:10.5194/acp-10-4273-2010, 2010.

Paytan, A. and McLaughlin, K.: The oceanic phosphorus cycle, Chem. Rev., 107, 563–576, 2007.

Quan, J., Tie, X., Zhang, Q., Liu, Q., Li, X., Gao, Y., and Zhao, D.: Characteristics of heavy aerosol pollution during the 2012–2013 winter in Beijing, China, Atmos. Environ., 88, 83–89, 2014.

Title Page

Abstract | Introduction

Conclusions | References

Tables | Figures

|◄ | ►|

◄ | ►

Back | Close

Full Screen / Esc

Printer-friendly Version

Interactive Discussion

Rubasinghege, G., Lentz, R. W., Scherer, M. M., and Grassian, V. H.: Simulated atmospheric processing of iron oxyhydroxide minerals at low pH: roles of particle size and acid anion in iron dissolution, P. Natl. Acad. Sci. USA, 107, 6628–6633, 2010.

Rubin, M., Berman-Frank, I., and Shaked, Y.: Dust- and mineral-iron utilization by the marine dinitrogen-fixer Trichodesmium, Nat. Geosci., 4, 529–534, 2011.

Salam, A., Bauer, H., Kassin, K., Ullah, S. M., and Puxbaum, H.: Aerosol chemical characteristics of a mega-city in Southeast Asia (Dhaka–Bangladesh), Atmos. Environ., 37, 2517–2528, 2003.

Schmidl, C., Marr, I. L., Caseiro, A., Kotianová, P., Berner, A., Bauer, H., Kasper-Giebl, A., and Puxbaum, H.: Chemical characterisation of fine particle emissions from wood stove combustion of common woods growing in mid-European Alpine regions, Atmos. Environ., 42, 126–141, 2008.

Schroth, A. W., Crusius, J., Sholkovitz, E. R., and Bostick, B. C.: Iron solubility driven by speciation in dust sources to the ocean, Nat. Geosci., 2, 337–340, 2009.

Sedwick, P. N., Sholkovitz, E. R., and Church, T. M.: Impact of anthropogenic combustion emissions on the fractional solubility of aerosol iron: evidence from the Sargasso Sea, Geochem. Geophy. Geosy., 10, Q10Q06, doi:10.1029/2007GC001586, 2007.

Seinfeld, J., Carmichael, G., Arimoto, R., Conant, W., Brechtel, F., Bates, T., Cahill, T., Clarke, A., Doherty, S., Flatau, P., Huebert, B., Kim, J., Markowicz, K., Quinn, P., Russell, L., Russell, P., Shimizu, A., Shinozuka, Y., Song, Ch., Tang, Y., Uno, I., Vogelmann, A., Weber, R., Woo, J., and Zhang, X.: ACE-ASIA: regional climatic and atmospheric chemical effects of Asian dust and pollution, B. Am. Meteorol. Soc., 85, 367–380, 2004.

Shi, Z., Krom, M. D., Bonneville, S., Baker, A. R., Bristow, C., Drake, N., Mann, G., Carslaw, K., McQuaid, J. B., Jickells, T., and Benning, L. G.: Influence of chemical weathering and aging of iron oxides on the potential iron solubility of Saharan dust during simulated atmospheric processing, Global Biogeochem. Cy., 25, GB2010, doi:10.1029/2010GB003837, 2011a.

Shi, Z., Bonneville, S., Krom, M. D., Carslaw, K. S., Jickells, T. D., Baker, A. R., and Benning, L. G.: Iron dissolution kinetics of mineral dust at low pH during simulated atmospheric processing, Atmos. Chem. Phys., 11, 995–1007, doi:10.5194/acp-11-995-2011, 2011b.

Shi, Z., Krom, M. D., Jickells, T. D., Bonneville, S., Carslaw, K. S., Mihalopoulos, N., Baker, A. R., and Benning, L. G.: Impacts on iron solubility in the mineral dust by processes in the source region and the atmosphere: a review, Aeolian Res., 5, 21–42, 2012.

Title Page

Abstract | Introduction

Conclusions | References

Tables | Figures

Back | Close

Full Screen / Esc

Printer-friendly Version

Interactive Discussion

Sholkovitz, E. R., Sedwick, P. N., and Church, T. M.: Influence of anthropogenic combustion emissions on the deposition of soluble aerosol iron to the ocean: empirical estimates for island sites in the North Atlantic, Geochim. Cosmochim. Ac., 73, 3981–4003, 2009.

Sholkovitz, E. R., Sedwick, P. N., Church, T. M., Baker, A. R., and Powell, C. F.: Fractional solubility of aerosol iron: synthesis of a global-scale data set, Geochim. Cosmochim. Ac., 89, 173–189, 2012.

Solmon, F., Chuang, P. Y., Meskhidze, N., and Chen, Y.: Acidic processing of mineral dust iron by anthropogenic compounds over the north Pacific Ocean, J. Geophys. Res., 114, D02305, doi:10.1029/2008JD010417, 2009.

Srinivas, B. and Sarin, M. M.: Atmospheric pathways of phosphorous to the Bay of Bengal: contribution from anthropogenic sources and mineral dust, Tellus B, 64, 17174, doi:10.3402/tellusb.v64i0.17174, 2012.

Sullivan, R. C., Guazzotti, S. A., Sodeman, D. A., and Prather, K. A.: Direct observations of the atmospheric processing of Asian mineral dust, Atmos. Chem. Phys., 7, 1213–1236, doi:10.5194/acp-7-1213-2007, 2007.

Takahashi, Y., Higashi, M., Furukawa, T., and Mitsunobu, S.: Change of iron species and iron solubility in Asian dust during the long-range transport from western China to Japan, Atmos. Chem. Phys., 11, 11237–11252, doi:10.5194/acp-11-11237-2011, 2011.

Taylor, S. R.: Abundance of chemical elements in the continental crust: a new table, Geochim. Cosmochim. Ac., 28, 1237–1285, 1964.

Toboa, Y., Zhang, D., Matsuki, A., and Iwasaka, Y.: Asian dust particles converted into aqueous droplets under remote marine atmospheric conditions, P. Natl. Acad. Sci. USA, 107, 17905–17910, 2010.

Trapp, J. M., Millero, F. J., and Prospero, J. M.: Trends in the solubility of iron in dustdominated aerosols in the equatorial Atlantic trade winds: importance of iron speciation and sources, Geochem. Geophy. Geosy., 11, Q03014, doi:10.1029/2009GC002651, 2010.

Wang, G., Huang, L., Gao, S., Gao, S., and Wang, L.: Characterization of water-soluble species of PM_{10} and $PM_{2.5}$ aerosols in urban area in Nanjing, China, Atmos. Environ., 36, 1299–1307, 2002.

Watson, J. G., Chow, J. C., and Houck, J. E.: $PM_{2.5}$ chemical source profiles for vehicle exhaust, vegetative burning, geological material, and coal burning in Northwestern Colorado during 1995, Chemosphere, 43, 1141–1151, 2001.

Title Page

Abstract | Introduction

Conclusions | References

Tables | Figures

|◄ | ►|

◄ | ►

Back | Close

Full Screen / Esc

Printer-friendly Version

Interactive Discussion

Wong, G. T. F., Chung, S. W., Shiah, F. K., Chen, C. C., Wen, L. S., and Liu, K. K.: Nitrate anomaly in the upper nutricline in the northern South China Sea – evidence for nitrogen fixation, Geophys. Res. Lett., 29, 2097, doi:10.1029/2002GL015796, 2002.

Wu, J. F., Chung, S. W., Wen, L. S., Liu, K. K., Chen, Y. L. L., Chen, H. Y., and Karl, D. M.: Dissolved inorganic phosphorus, dissolved iron, and Trichodesmium in the oligotrophic South China Sea, Global Biogeochem. Cy., 17, 1008, doi:10.1029/2002GB001924, 2003.

Zhang, D. Z. and Iwasaka, Y.: Nitrate and sulfate in individual Asian dust-storm particles in Beijing, China in spring of 1995 and 1996, Atmos. Environ., 33, 3213–3223, 1999.

Zhang, D. Z. and Iwasaka, Y.: Chlorine deposition on dust particles in marine atmosphere, Geophys. Res. Lett., 28, 3613–3616, 2001.

Zhang, R., Jing, J., Tao, J., Hsu, S.-C., Wang, G., Cao, J., Lee, C. S. L., Zhu, L., Chen, Z., Zhao, Y., and Shen, Z.: Chemical characterization and source apportionment of $PM_{2.5}$ in Beijing: seasonal perspective, Atmos. Chem. Phys., 13, 7053–7074, doi:10.5194/acp-13-7053-2013, 2013.

Zhu, X. R., Prospero, J. M., and Millero, F. J.: Diel variability of soluble Fe(II) and soluble total Fe in North African dust in the trade winds at Barbados, J. Geophys. Res., 102, 21297–21305, doi:10.1029/97JD01313, 1997.

Zhuang, G. S., Yi, Z., and Duce, R. A.: Brown PR Link between iron and sulfur cycles suggested by detection of Fe (II) in remote marine aerosols, Nature, 355, 537–539, 1992.

Sources, solubility, and acid processing of aerosol iron and phosphorous over the South China Sea

S.-C. Hsu et al.

Table 1. Statistical summary (mean ± standard deviation, and range) of the data on fractional Al, Fe, and P solubility (%Al, %Fe, and %P) along with atmospheric concentrations ($ng\,m^{-3}$) of selected aerosol species. Data for the June cruise are considered with two cases, i.e., one case included all samples ($n = 17$) and the other excluded three samples ($n = 14$) not influenced by Indonesian biomass burning.

| | Feb–Mar ($n = 18$) | | Jun ($n = 17$) | | Jun ($n = 14$) | |
	Mean ± S.D.	Range	Mean ± S.D.	Range	Mean ± S.D.	Range
%Al	6.5 ± 3.5	2.1–15	3.7 ± 2.6	0.7–11.5	3.2 ± 1.9	0.7–7.2
%Fe	11 ± 5.3	3.6–21	3.0 ± 2.2	1.4–8.2	2.5 ± 1.5	1.4–6.3
%P	55 ± 14	31–81	45 ± 17	9.3–90	50 ± 14	20–90
Al_T	212 ± 470	56–1486	1193 ± 1161	109–3475	1963 ± 914	534–3475
Fe_T	205 ± 334	63–1159	756 ± 709	70–2162	1212 ± 559	317–2162
P_T	10 ± 11	4.2–44	36 ± 22	9.5–79	44 ± 19	18–79
Al_S	14 ± 10	6.5–35	44 ± 41	7.1–172	63 ± 37	9.3–172
Fe_S	23 ± 17	11–56	23 ± 19	4.2–86	31 ± 17	12–86
P_S	5.6 ± 4.7	2.3–20	16 ± 12	0.9–41	22 ± 10	6.7–41
$nss\text{-}K^+$	269 ± 118	82–499	179 ± 180	12–690	262 ± 161	57–690
$nss\text{-}SO_4^{2-}$	6553 ± 3783	2861–14 457	3013 ± 1777	693–8066	3681 ± 1570	1391–8066
NO_3^-	3405 ± 2115	1750–11 220	2744 ± 1324	463–5710	3351 ± 1039	1574–5710
NH_4^+	2057 ± 1158	960–5681	1220 ± 993	332–4696	1389 ± 1005	428–4696
Cl^-	9498 ± 4706	2480–17 946	4329 ± 6820	1544–19 961	4458 ± 7380	1544–19 961
Na^+	6812 ± 2858	2164–12 086	2418 ± 4072	749–12 330	2425 ± 4431	749–12 330
Mg^{2+}	805 ± 342	315–1465	391 ± 436	161–1375	427 ± 464	193–1375
K^+	541 ± 182	238–948	339 ± 234	67–1061	422 ± 216	256–1061
Ca^{2+}	442 ± 262	124–1003	1129 ± 883	129–3060	1677 ± 674	724–3060
SO_4^{2-}	8514 ± 4004	3651–17 478	4081 ± 2032	1278–10 567	4789 ± 1819	3766–10 567

Table 2a. Correlation matrix between selected aerosol species for the Feb–Mar cruise samples. The coefficients for the correlations of Fe_T, P_T, Fe_S, and P_S against Al_T, $nss\text{-}SO_4^{2-}$, and $nss\text{-}K^+$ are underlined (Figs. 6 and 7).

(n = 18)	Al_T	Fe_T	P_T	Al_S	Fe_S	P_S	$nss\text{-}K^+$	$nss\text{-}SO_4^{2-}$	NO_3^-	NH_4^+	Cl^-	Na^+
Al_T	1											
Fe_T	0.992	1										
P_T	0.960	0.974	1									
Al_S	0.838	0.854	0.767	1								
Fe_S	0.737	0.757	0.668	0.975	1							
P_S	0.921	0.949	0.961	0.840	0.757	1						
$nss\text{-}K^+$	0.593	0.645	0.576	0.873	0.883	0.678	1					
$nss\text{-}SO_4^{2-}$	0.592	0.626	0.544	0.914	0.950	0.663	0.919	1				
NO_3^-	0.807	0.848	0.885	0.634	0.508	0.902	0.467	0.428	1			
NH_4^+	0.732	0.790	0.771	0.796	0.711	0.864	0.745	0.712	0.888	1		
Cl^-	−0.512	−0.468	−0.515	−0.168	−0.060	−0.430	0.197	0.066	−0.523	−0.202	1	
Na^+	−0.434	−0.387	−0.438	−0.038	0.091	−0.338	0.321	0.223	−0.495	−0.148	0.978	1

Table 2b. Correlation matrix between selected aerosol species for the Jun cruise samples (excluding three samples). The coefficients for the correlations of Fe_T, P_T, Fe_S, and P_S against Al_T, $nss\text{-}SO_4^{2-}$, and $nss\text{-}K^+$ are underlined (Figs. 6 and 7).

$(n = 14)$	Al_T	Fe_T	P_T	Al_S	Fe_S	P_S	$nss\text{-}K^+$	$nss\text{-}SO_4^{2-}$	NO_3^-	NH_4^+	Cl^-	Na^+
Al_T	1											
Fe_T	0.999	1										
P_T	0.964	0.961	1									
Al_S	0.659	0.645	0.699	1								
Fe_S	0.607	0.595	0.657	0.977	1							
P_S	0.904	0.891	0.914	0.856	0.788	1						
$nss\text{-}K^+$	0.770	0.755	0.832	0.942	0.916	0.942	1					
$nss\text{-}SO_4^{2-}$	0.497	0.485	0.475	0.888	0.891	0.699	0.801	1				
NO_3^-	0.825	0.816	0.830	0.917	0.871	0.930	0.923	0.835	1			
NH_4^+	0.401	0.394	0.417	0.879	0.927	0.596	0.770	0.949	0.769	1		
Cl^-	−0.086	−0.073	0.003	0.079	0.204	−0.186	−0.050	−0.062	−0.035	0.184	1	
Na^+	−0.169	−0.157	−0.075	0.021	0.146	−0.258	−0.116	−0.110	−0.099	0.137	0.995	1

Figure 1. Maps of coarse (upper panel) and fine (lower panel) aerosol optical depth (AOD) distribution during the first cruise period (18 February to 8 March).
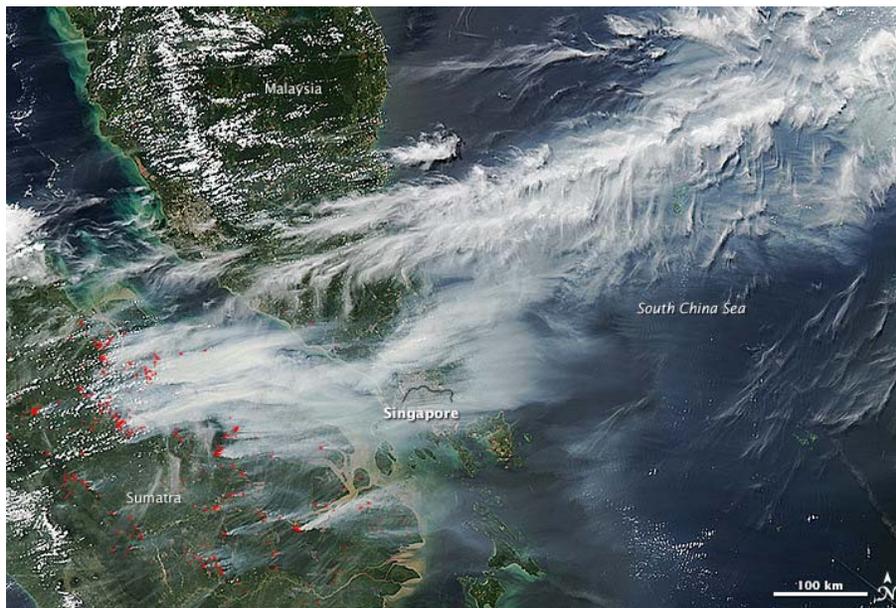
Figure 2. MODIS image of firing spots over Sumatra, Indonesia on 19 June 2013, showing that smoke blew east toward Malaysia and Singapore and farther the SCS, which was taken from http://earthobservatory.nasa.gov/IOTD/view.php?id=81431.

Full Screen / Esc

Printer-friendly Version

Interactive Discussion
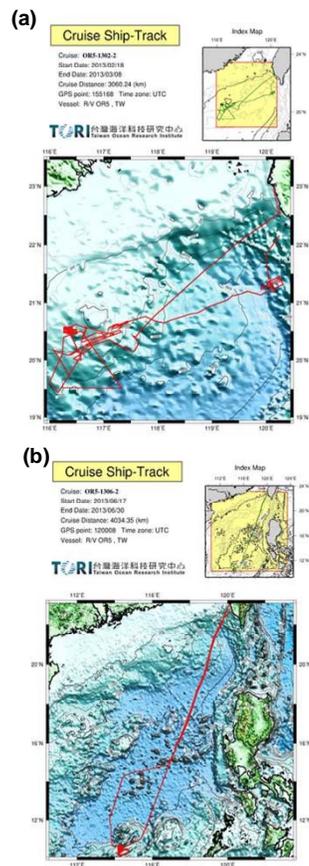
Figure 3. Maps showing ship tracks of the two sampling cruises of R/V *OR5* over the SCS. The tracks were provided by Taiwan Ocean Research Institute (TORI), NARLabs. The exact collection locations of each sample are given in Table S1.
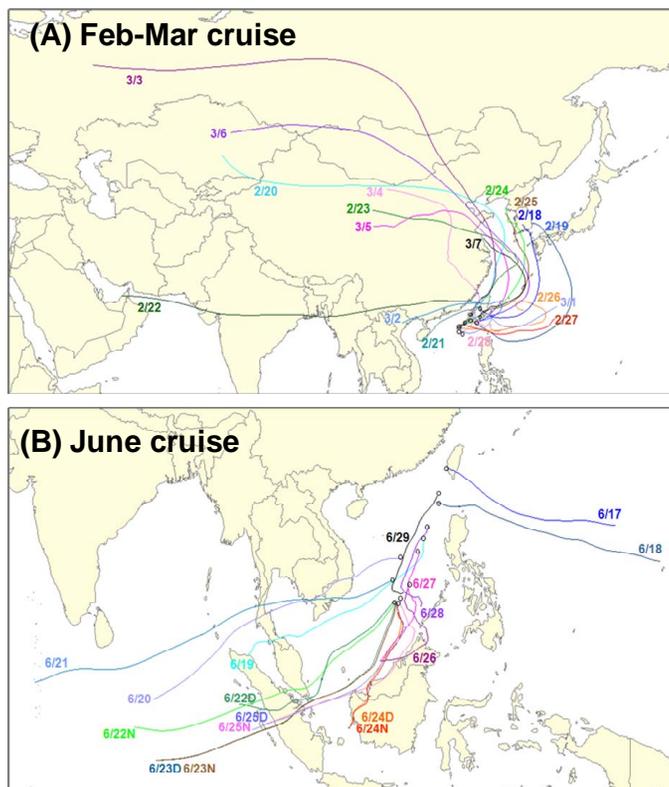
Figure 4. Five-day back trajectories at 500 m above mean sea level correspondent to each sample, whose initial locations were set at the beginning sampling location and time of each sample.

Title Page

Abstract | Introduction

Conclusions | References

Tables | Figures

|◄ | ►|

◄ | ►

Back | Close

Full Screen / Esc

Printer-friendly Version

Interactive Discussion
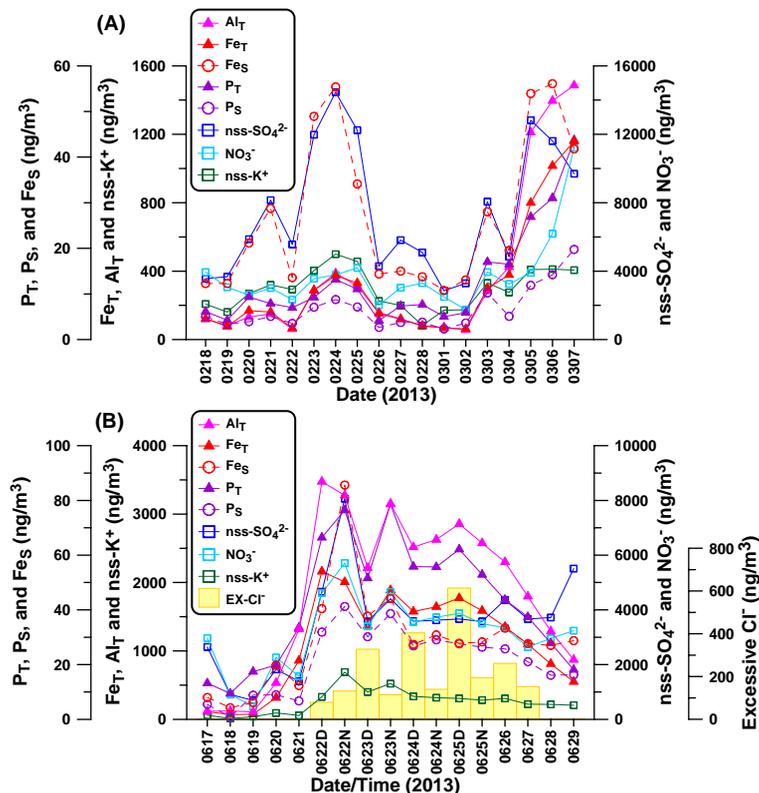
Figure 5. Time-series of water-soluble Fe and P (Fe_S and P_S) and total Fe and P (Fe_T and P_T) along with total Al (Al_T), non-sea salt sulfate (nss-SO_4^{2-}), non-sea salt potassium (nss-K^+) and NO_3^- in marine aerosols collected from two cruises over the SCS in 2013: **(A)** 18 February to 7 March ($n = 18$) and **(B)** 17 to 29 June ($n = 17$). Excessive chloride (EX-Cl^-) is also shown in **(B)**, and defined in the text.

Discussion Paper | Discussion Paper | Discussion Paper | Discussion Paper |

ACPD

14, 21433–21472, 2014

Sources, solubility, and acid processing of aerosol iron and phosphorous over the South China Sea

S.-C. Hsu et al.

Title Page	
Abstract	Introduction
Conclusions	References
Tables	Figures

|◄	►|
◄	►

Back	Close

Full Screen / Esc

Printer-friendly Version

Interactive Discussion
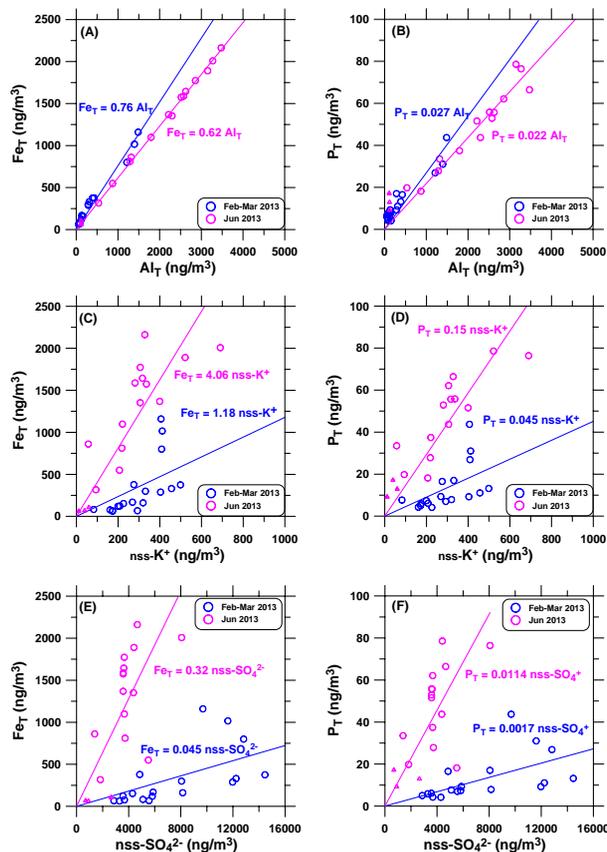
Figure 6. Correlations of **(A)** Fe_T against Al_T, **(B)** P_T against Al_T, **(C)** Fe_T against nss-K^+, **(D)** P_T against nss-K^+, **(E)** Fe_T against nss-SO_4^{2-}, and **(F)** P_T against nss-SO_4^{2-} in the SCS marine aerosols. Also shown are the regression lines forced to origin, along with the regression equations.

Title Page

Abstract | Introduction

Conclusions | References

Tables | Figures

|◀ | ▶|

◀ | ▶

Back | Close

Full Screen / Esc

Printer-friendly Version

Interactive Discussion
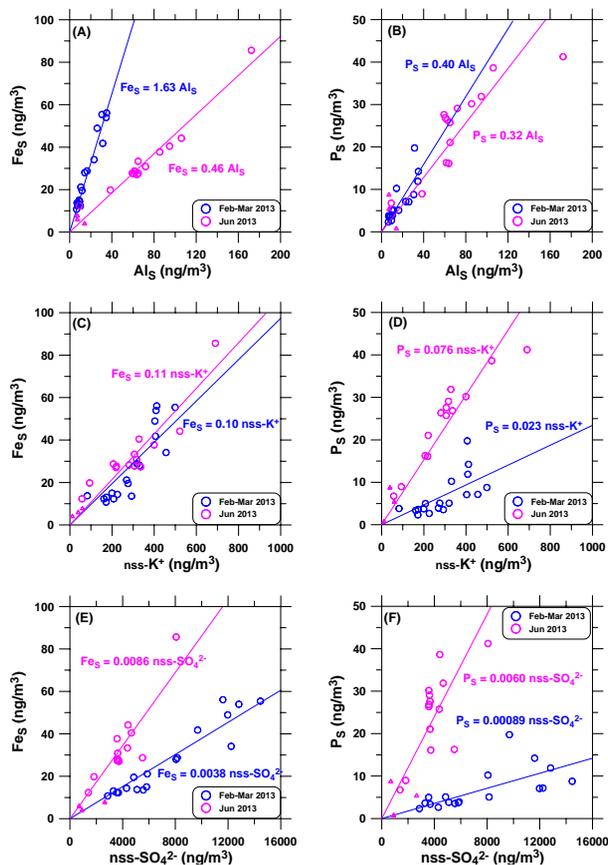
Figure 7. Correlations of **(A)** Fe_S against Al_T, **(B)** P_S against Al_T, **(C)** Fe_S against nss-K^+, **(D)** P_S against nss-K^+, **(E)** Fe_S against nss-SO_4^{2-}, and **(F)** P_S against nss-SO_4^{2-} in the SCS marine aerosols. Also shown are the regression lines forced to origin, along with the regression equations.

Title Page

Abstract | Introduction

Conclusions | References

Tables | Figures

|◀ | ▶|

◀ | ▶

Back | Close

Full Screen / Esc

Printer-friendly Version

Interactive Discussion
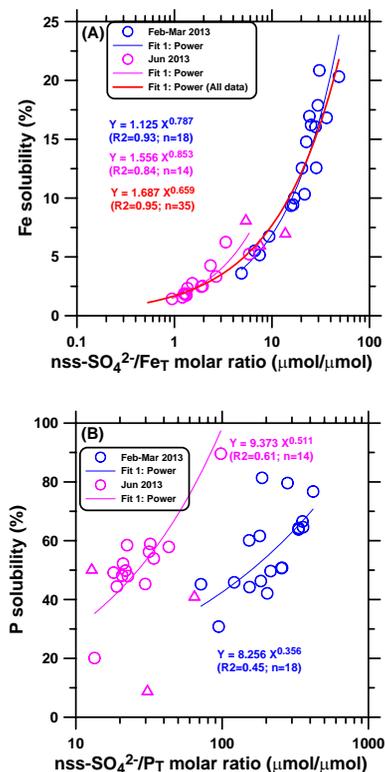
Figure 8. Relationships of **(A)** fractional Fe solubility (%Fe) against Fe_T/nss-sulfate molar ratios and **(B)** fractional P solubility (%P) against P_T/nss-sulfate molar ratio. Also shown are the best regression curves along with regression equations by considering the data from individual cruises and the combination of these data.

Title Page

Abstract | Introduction

Conclusions | References

Tables | Figures

|◄ | ►|

◄ | ►

Back | Close

Full Screen / Esc

Printer-friendly Version

Interactive Discussion

Discussion Paper | Discussion Paper | Discussion Paper | Discussion Paper

ACPD

14, 21433–21472, 2014

Sources, solubility, and acid processing of aerosol iron and phosphorous over the South China Sea

S.-C. Hsu et al.

Title Page

Abstract	Introduction
Conclusions	References
Tables	Figures

|◄   ►|

◄   ►

Back   Close

Full Screen / Esc

Printer-friendly Version

Interactive Discussion
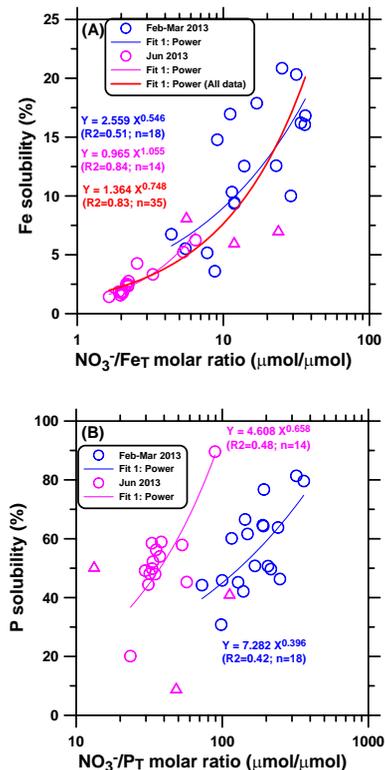
Figure 9. Relationships of **(A)** fractional Fe solubility (%Fe) against Fe_T/nitrate molar ratios and **(B)** fractional P solubility (%P) against P_T/nitrate molar ratio. Also shown are the best regression curves along with regression equations by considering the data from the individual cruises and the combination of these data.
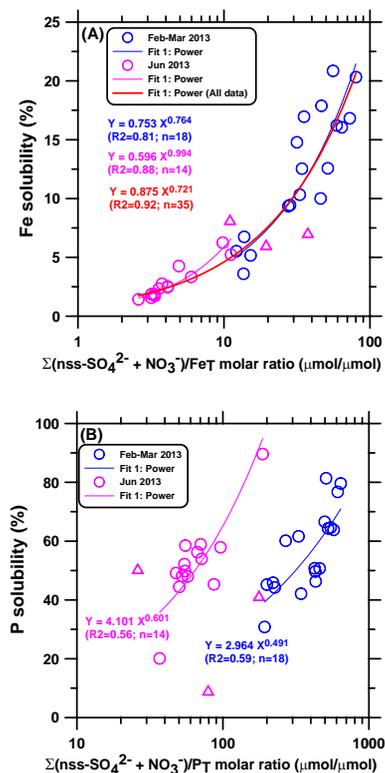
Figure 10. Relationships of **(A)** fractional Fe solubility (%Fe) against Fe_T/Σ (nss-SO_4^{2-}, NO_3^-) molar ratios and **(B)** fractional P solubility (%P) against P_T/Σ (nss-SO_4^{2-}, NO_3^-) molar ratio. Also shown are the best regression curves along with regression equations by considering the data from individual cruises and the combination of these data.

Full Screen / Esc

Printer-friendly Version

Interactive Discussion